Available online at www.sciencedirect.com

SciVerse ScienceDirect

Ceramics International 39 (2013) 5151–5158

CERAMICS INTERNATIONAL

www.elsevier.com/locate/ceramint

Low-fire processing of microwave $BaTi_4O_9$ dielectric with crystalline CuB_2O_4 and $BaCuB_2O_5$ additives

Yung-Ju Chu, Jau-Ho Jean*

Department of Materials Science and Engineering, National Tsing Hua University, 101 Section 2, Kuang Fu Road, Hsinchu, Taiwan

Received 2 November 2012; received in revised form 2 December 2012; accepted 5 December 2012
Available online 23 December 2012

Abstract

The effects of interfacial reaction of CuB_2O_4 (CB)/$BaTi_4O_9$ (BT4) and $BaCuB_2O_5$ (BCB)/$BaTi_4O_9$ (BT4) on densification, phase development and dielectric properties of $BaTi_4O_9$ (BT4) have been investigated. With BaO present, the wetting of BCB/BT4 improves significantly in comparison to CB/BT4 at temperatures below 925 °C. However, the enhancement in densification becomes less significant for BCB + BT4 than that of CB + BT4 at reduced temperatures. The above results are attributed to a chemical reaction taking place at the interface of CB/BT4 and BCB/BT4 during firing, which becomes less extensive with BaO present in the sintering promoter. For both CB + BT4 and BCB + BT4 systems, the resulting composites have a dielectric constant of 36–40, product ($Q \cdot f_r$) of quality factor (Q) and resonant frequency (f_r) of 13,000–21,000 GHz, and a temperature coefficient of resonant frequency (τ_f) of 20–40 ppm/°C in the temperature range of 25–80 °C.

Keywords: Dielectric; Microwave; Low-temperature cofired ceramics (LTCC)

1. Introduction

Wireless communication ceramic devices have been extensively fabricated by a technology of low-temperature cofired ceramics (LTCC), because it provides outstanding characteristics such as reduced circuit dimension, high level of passive integration, exceptional high frequency performance, excellent reliability and low cost. Ceramic-filled glass (CFG) [1–3], glass-ceramics (crystallizable glass) [4–7] and low-fire crystalline compounds [8–17] have been commonly used to prepare LTCC systems. A mixture of low-softening-point glass and ceramic filler powders is prepared for the CFG method, where the low-softening-point glass is used to promote densification, and the ceramic fillers, to adjust the physical properties of the resulting composites. For the approach of glass-ceramics, a pure glass powder that forms crystalline phases during firing is used as a starting material. Physical properties of the resulting glass + ceramic composite are controlled by the characteristics and amount of crystalline phases formed. For the method of low-fire crystalline compounds [8–17], compounds including Bi_2O_3–TeO_2, TiO_2–TeO_2, CaO–TeO_2, BaO–TeO_2, ZnO–TeO_2, BaO–TiO_2–TeO_2, Bi_2O_3–MoO_3 and Bi_2O_3–WO_3 systems that can be densified at 600–800 °C and exhibit promising microwave properties are used. Because of its ease in processing and simplicity to tune the physical properties of fired ceramic composites, the CFG method is preferred in the LTCC industry. Since the added glass in the CFG method has a low dielectric constant and quality factor, it deteriorates the dielectric properties of the resulting composites significantly. To minimize it, a crystalline solid that reacts with ceramic fillers during firing is investigated in this study. $BaTi_4O_9$ (BT4) is chosen as the ceramic filler because of its excellent microwave dielectric properties, i.e., a dielectric constant of approximately 37–39, and product ($Q \cdot f_r$) of quality factor (Q) and resonant frequency (f_r) of 22,700 GHz [18–21]. A high sintering temperature, e.g., 1300 °C, is required to densify BT4, which, however, limits its use to cofire with high-electrical-conductivity but low-fire metallization of Ag or Cu. To lower the sintering temperature of BT4 dielectric below 950 °C, several methods including liquid-mixing process [22,23], and adding low-softening-point glass or liquid-phase-sintering aid have been reported [24–32]. In this investigation, the approach

---

*Corresponding author. Tel.: +886 3 5719921.
E-mail address: jhjean@mse.nthu.edu.tw (J.-H. Jean).

0272-8842/$ - see front matter © 2012 Elsevier Ltd and Techna Group S.r.l. All rights reserved.
http://dx.doi.org/10.1016/j.ceramint.2012.12.011

of adding a small amount of crystalline phase of CuB_2O_4 (CB) and $BaCuB_2O_5$ (BCB) to BT4 is taken. BaO is added to the CB to reduce its melting point, and to enhance chemical compatibility between BCB and BT4. The effects of CB and BCB content on the densification, phase development and dielectric properties of BT4 ceramics are investigated.

2. Experimental procedure

$BaTi_4O_9$ (BT4) powder was prepared using high-purity powders of $BaCO_3$ (J.T. Baker, Phillipsburg, NJ) and TiO_2 (Showa, Japan), which were mixed, dried and calcined at 1100 °C for 3 h. The calcined powders were ball-milled in 1-propanol with zirconia media for 120 h. The resulting powder had a median size of 0.25 μm measured by light scattering analysis (Coulter Counter, USA). X-ray diffraction (XRD) result showed a pure crystalline phase of BT4 without residual reactant phases. The BT4 compact was then pressed and fired at 1350 °C for 2 h, which gave a relative sintered density of 99%, dielectric constant of 38, $Q \cdot f_r$ of 38,000 GHz at 6.6 GHz, and a temperature coefficient of resonant frequency (τ_f) of 20 ppm/°C in the temperature range of 25–80 °C.

For CuB_2O_4 (CB) powder, high-purity powders of CuO (Alpha, USA) and H_3BO_3 (Showa, Japan) were weighed, mixed and calcined at 850 °C for 3 h. The milled CB powder exhibited no extra phases and had a median particle size of 0.1 μm. To obtain a pure phase of $BaCuB_2O_5$ (BCB) powder, the powder was synthesized by a wet chemical reaction method [33]. High-purity H_3BO_3, $BaCO_3$, $Cu(NO_3)_2 \cdot 2.5H_2O$ (J.T. Baker, Phillipsburg, NJ) and citric acid (Sigma-aldrich, USA) were dissolved in de-ionized water. The clear solution was then heated under stirring at 80 °C. To remove water completely, the gel complex was dried at 180 °C for 48 h. The flurry black powder was then calcined at 700 °C for 3 h in air to remove the organics completely. XRD analysis showed a pure crystalline phase of BCB without residual reactant phases. The milled BCB powder had a median particle size of 0.07 μm.

The BT4 powder with different amounts of CB or BCB powder were mixed with 5 wt% poly(ethylene glycol) binder in 1-propanol. The suspension was deagglomerated using a high-energy ultrasonic horn, and mixing was continued using a Turbula mixer (Maschinenfabrik Basel, Switzerland) for 2 h. The powder mixture was dried, ground, and uniaxially pressed at approximately 90 MPa to make pellets of 1.3 cm diameter and 0.3 cm height. Samples with different CB or BCB contents were sintered isothermally in air at 875–925°C for 2 h. Crystalline phases of the sintered samples were identified by XRD. Sintered densities were measured by the water replacement method. Samples were immersed in water, and the open pores were filled with water in vacuum for 2 h. The apparent bulk density used to calculate the relative sintered density of sintered compacts was determined with a He pycnometer using the powders prepared by grinding the sintered compacts. For the experiments of thermo-mechanical analyses (TMA) (Seiko Instruments, Japan), samples were fired at a heating rate of 5 °C/min in flowing air. Wetting behavior of CB/BT4 and BCB/BT4 was studied by placing a piece of green CB or BCB compact on top of dense BT4 substrate and fired at a heating rate of 10 °C/min from room temperature to 1100 °C to form a bond of CB/BT4 and BCB/BT4. Contact angle was recorded in-situ by a camera system. The interfacial reaction of CB/BT4 and BCB/BT4 was then investigated by a scanning electron microscopy (SEM), and elemental distributions were determined by EDX. Dielectric properties at microwave frequencies were determined by a method developed by Hakki and Coleman [34], and Kobayashi and Katoh [35] using a network analyzer (8722D, Agilent, USA).

3. Results and discussion

Fig. 1 shows the wetting of CB/BT4 and BCB/BT4 at different temperatures. Since the melting point of CB is 1010 °C [36], no significant wetting between CB and BT4 is observed at temperatures below 925 °C (Fig. 1(A)). Complete wetting with a negligible contact angle is observed at temperatures above 1035 °C. For BCB (Fig. 1(B)), partial wetting with a contact angle around 45° at 900 °C and complete wetting with a negligible contact angle at 925 °C are observed because BCB has a melting point at 920–930 °C [37]. The above results also indicate an excellent chemical compatibility existing between BCB and BT4 at sintering temperatures of interest, i.e., 900–925 °C.

Fig. 2 shows the effects of CB and BCB content on shrinkage behavior of BT4. No significant shrinkage is observed for pure BT4 (Fig. 2(a)) and CB (Fig. 2(c)) at temperatures below 900 °C, which agrees with the observation in Fig. 1. For the system of BT4+0.34 vol% BCB (Fig. 2(b)), the shrinkage starts at 850 °C, and ends with a 6% linear shrinkage only at 1000 °C. Although the pure BCB can be fully densified at 790 °C [37], the binary composite of BT4+BCB still requires a sufficient amount of BCB to complete densification at 875–925 °C that is to be discussed in more details in Fig. 3. For the system with 0.34 vol% CB (Fig. 2(d)), however, the binary BT4+CB

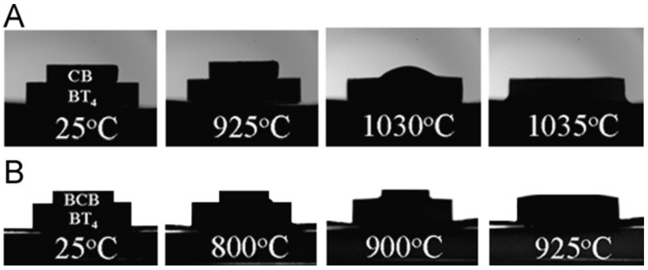

Fig. 1. Wetting behavior of (A) CB and (B) BCB on the BT4 substrate at different temperatures.

composite exhibits an onset sintering temperature of 775 °C, and a linear shrinkage of 17% at 1000 °C. Although the difference in final shrinkage becomes insignificant when the content of sintering additive increases up to 4.47 vol%, the shrinkage curve exhibits two stages for BT4+CB (Fig. 2(f)) but one stage for BT4+BCB (Fig. 2(e)). At the first stage of sintering, i.e., 650–775 °C, the system with 4.47 vol% CB has a linear shrinkage of 6–7% which is much larger than that with 4.47 vol% BCB, 1–2%, as shown in Fig. 2. No significant difference in shrinkage behavior for both systems at temperatures above 850–875 °C. The above results clearly indicate that although the CB exhibits poorer wetting on BT4 below 925 °C, but larger and faster densification than that with BCB at a given temperature. These observations are further supported by the densification results in Fig. 3, where the binary composites with different amounts of CB or BCB are fired at 875–925 °C for 2 h. For both systems, the densification increases with increasing CB or BCB content at a given temperature. At a given sintering additive content, however, a larger densification is always observed for the binary composite with CB than BCB, and the difference becomes more significant at reduced sintering temperatures. To achieve a relative sintered density above 98%, 0.34 vol% CB in relative to 1 vol% BCB at 925 °C, and 3.35 vol% CB compared with 4.47 vol% BCB at 900 °C is required. For comparison, little densification

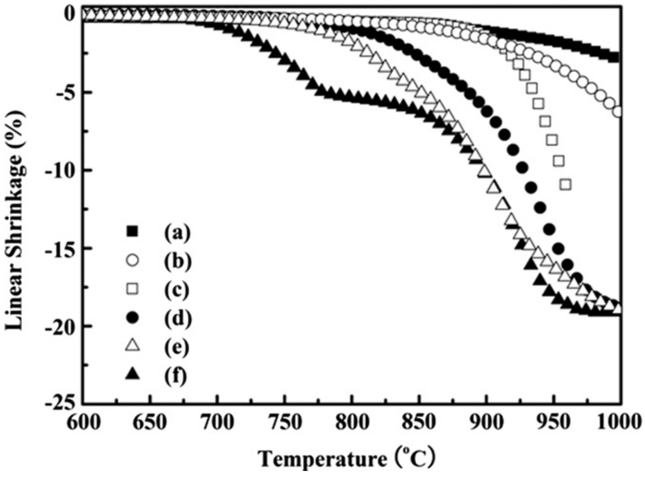

Fig. 2. Linear shrinkage curves of (a) BT4, (b) BT4+0.34 vol% BCB, (c) CB, (d) BT4+0.34 vol% CB, (e) BT4+4.47 vol% BCB and (f) BT4+4.47 vol% CB at a heating rate of 5 °C/min in air.

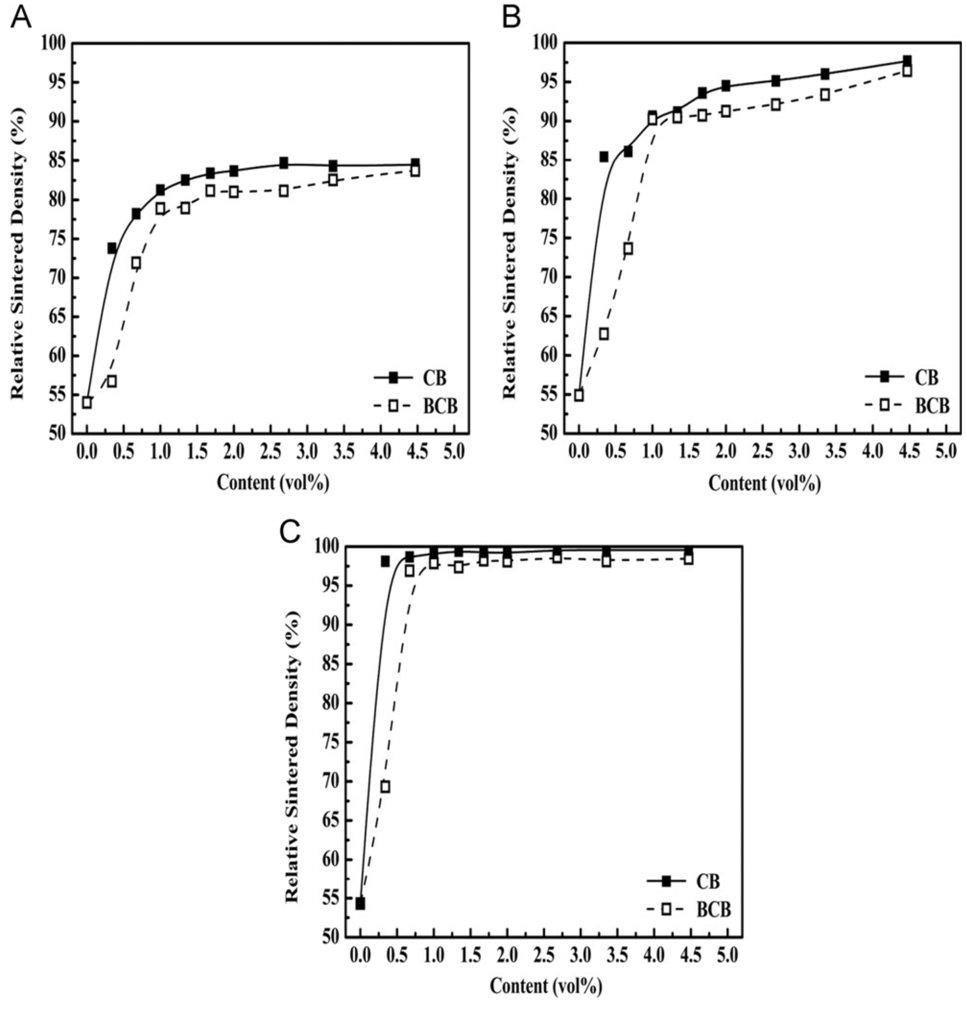

Fig. 3. Effects of CB and BCB content on densification of BT4 at (A) 875, (B) 900 and (C) 925 °C, for 2 h.

with a relative sintered density of 55–58% for pure BT4 is measured under the same firing conditions. These results are further evidenced by comparing microstructures of the samples with 0.34 vol% CB and BCB, as shown in Fig. 4. Porous microstructure is observed in the binary composite with 0.34 vol% BCB (Fig. 4(A)), but a dense and uniform microstructure with a relative sintered density greater than 98% is obtained with 0.34 vol% CB (Fig. 4(B)).

Effects of the sintering additives on phase development of the binary composites are summarized in Fig. 5. For the BT4+BCB system (Fig. 5(A)), only crystalline phases of BT4 and $Ba_4Ti_{13}O_{30}$ (B4T13) are found for all compositions investigated. No crystalline BCB phase is detected because BCB melts or reacts with BT4 completely to form an amorphous BaO–CuO–B_2O_3 phase during sintering. This is confirmed by SEM/EDX observations in Fig. 6(A), where BT4 exhibits granular, rhombus and triangle shapes, and B4T13, rectangle shape. The Residual BaO–CuO–B_2O_3 phases, which are located at the corner of grain boundaries, are also detected. The crystallization behavior becomes more complicated with CB present, as shown in Fig. 5(B) where new phases including $Ba_2Ti_9O_{20}$ (B2T9), $BaTi_5O_{11}$ (BT5), $Ba_4Ti_{13}O_{30}$ (B4T13), and $BaTi(BO_3)_2$ (BTB) are found. Again, no crystalline CB phase is found. SEM/EDX examination also supports the above observation, as shown in Fig. 6(B) at which granular BT4, bar-shaped BT5 and rectangle-shaped B4T13 are identified. Newly formed amorphous BaO–CuO–B_2O_3 phases are detected at the corner of grain boundaries. No BTB grain is found, which might be due to its small sizes. At all conditions investigated, the amount of new phases formed except B2T9 increases but the residual BT4 decreases with increasing BCB and CB content, which is semi-quantitatively supported by the peak intensity ratio of X-phase/($BT4_{(121)}+B2T9(\bar{2}20)+BT5_{(041)}+B4T13_{(113)}+BTB_{(104)}$) in Fig. 7(A) and (B), respectively. Note that the X-phase is $BT4_{(121)}$, $B2T9(\bar{2}20)$, $BT5_{(041)}$, $B4T13_{(113)}$, or $BTB_{(104)}$. Careful examination of the XRD results in Fig. 7 finds that the amount of residual BT4 decreases much more significantly with CB (Fig. 7(B)) than BCB (Fig. 7(A)). For example, 100% and 85% for 0.34 vol% BCB and CB, 80% and 30% for 0.67 vol% BCB and CB, and 60% and 10%

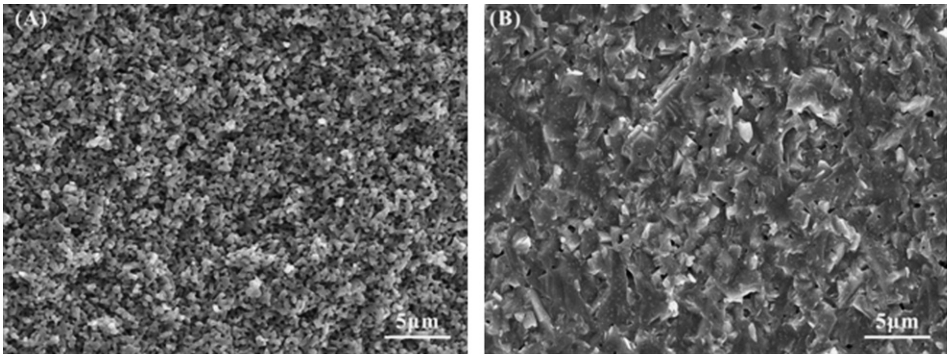

Fig. 4. Microstructure of (A) BT4+0.34 vol% BCB and (B) BT4+0.34 vol% CB fired at 925 °C for 2 h.

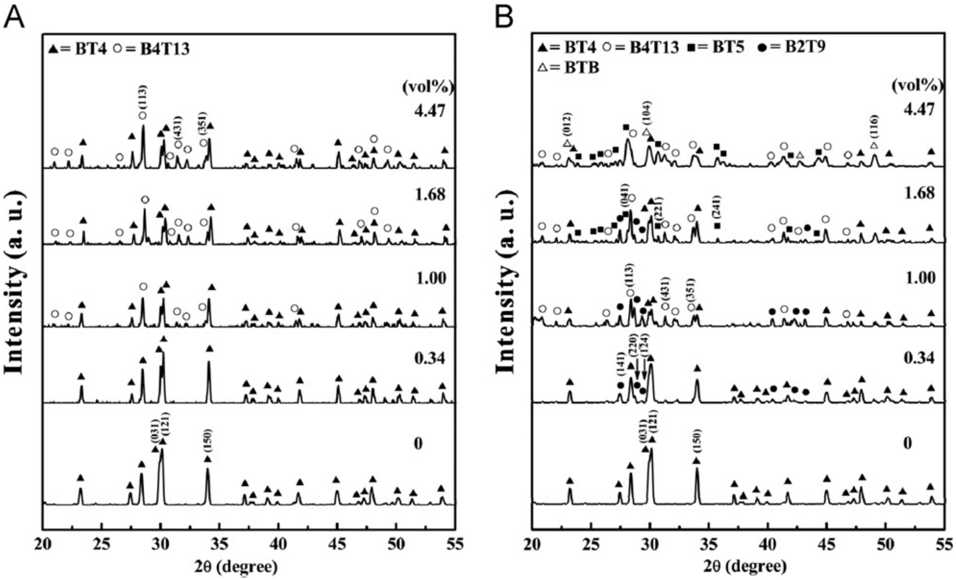

Fig. 5. Effects of (A) BCB and (B) CB contents on the formation of new phases during firing BT4 composites at 925 °C, for 2 h.

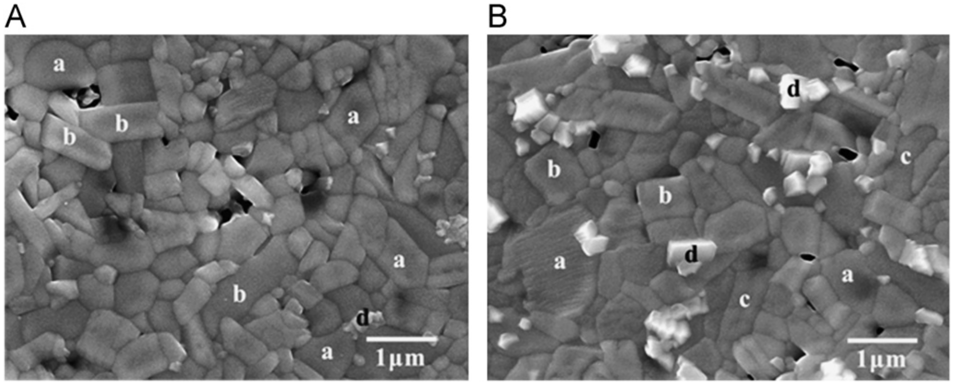

Fig. 6. Microstructure and phase identification of BT4 with 3.35 vol% (A) BCB and (B) CB fired at 925 °C, for 2 h. Grains a, b, c, and d are BT4, B4T13, BT5 and amorphous BaO-CuO-B_2O_3, respectively.

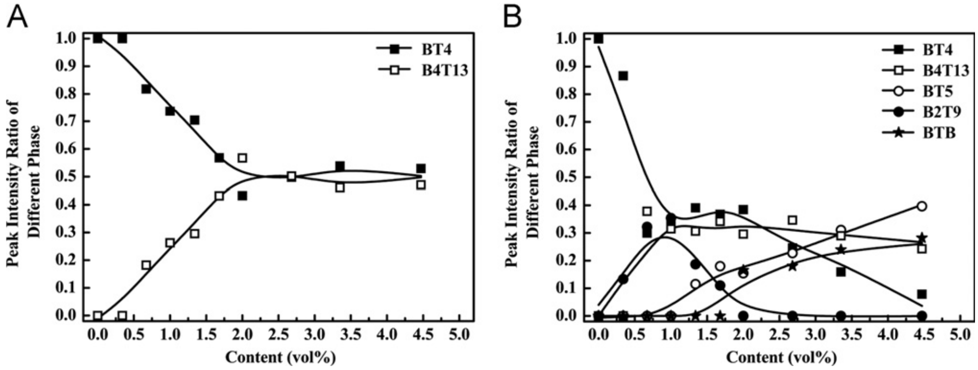

Fig. 7. XRD peak intensity ratio of different phases for BT4 with different amounts of (A) BCB and (B) CB fired at 925 °C, for 2 h.

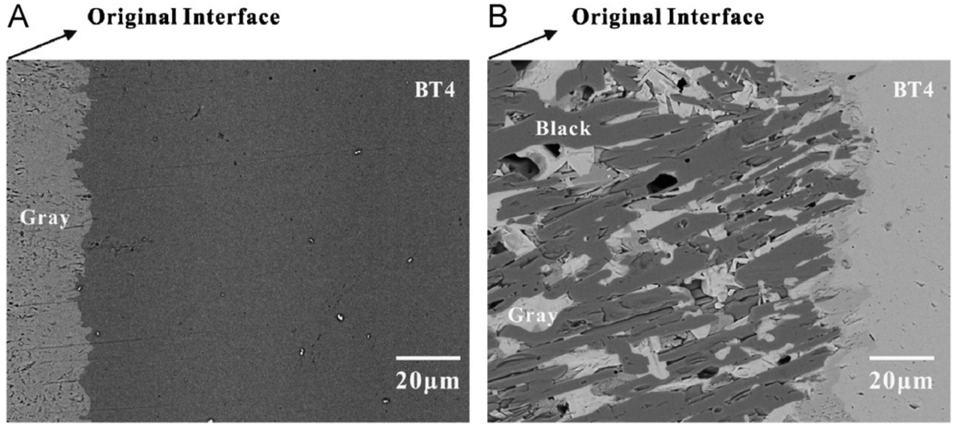

Fig. 8. Microstructure of reaction layer formed on BT4 side during firing (A) BCB/BT4 and (B) CB/BT4 diffusion couple at 925 °C, for 2 h.

for 4.47 vol% BCB and CB, respectively. Results in Figs. 1 and 7 clearly indicate that although the BaO in the BCB improves the wetting between BCB and BT4 at elevated temperatures (Fig. 1(B)), it diminishes the chemical reaction between BT4 and BCB during sintering. This in turn minimizes new phases formed, and reduces the densification of BT4+BCB (Figs. 2 and 3). The above inference is confirmed by the interfacial reaction of CB/BT4 and BCB/BT4 at 925 °C, as shown in Fig. 8. A gray reaction layer, which can be identified in the SEM micrograph (Fig. 8(A)) based upon image contrast, is found on BT4 side in the system of BCB/BT4. EDX results show that compared with pure BT4, the gray region is Ba-rich Ba–Ti oxide. For the CB/BT4 system (Fig. 8(B)), however, a two-phase reaction layer including gray Ba-rich Ba–Ti oxide and black Ti-rich Ba–Ti oxide regions is formed. Results of reaction layer thickness on BT4 side as a function of time are summarized in Fig. 9, where a thicker reaction layer is always found in the system of CB/BT4 than BCB/BT4. The above results clearly indicate that although the presence of BaO in the BCB improves the wetting between BCB and BT4 at elevated temperatures (Fig. 1), it minimizes the chemical reaction between BCB and BT4. This results in a less reactive liquid-phase sintering taking place in BCB/BT4 than CB/BT4 during firing.

The effects of CB and BCB content on dielectric properties of BT4 are shown in Fig. 10, where no significant difference between BT4+CB and BT4+BCB is noticed.

The dielectric constant (k) at 6.6 GHz (Fig. 10(A)) varies in the range of 36–40, and exhibits an increasing trend with increasing CB or BCB content in the range of 0.34–1.0 vol%. This is a result of increasing densification with increasing CB or BCB content (Fig. 3). Beyond that, no significant change in dielectric constant with CB or BCB content is observed. This might be due to the low dielectric constant of CB (k=6–7) and BCB (k=7–8) [37] as the k values of BT4, BT5, B2T9, and B4T13 are in the similar range of 38–42 [18,31,38–41]. Results of the product ($Q\cdot f_r$) of quality factor (Q) and resonant frequency (f_r) are also shown in Fig. 10(B), which are in the range of 13,000–21,000 GHz and smaller than those of pure BT4, BT5 and B2T9, 32,000–46,000 GHz [18,38,39,41]. This is caused by the dilution effect of low-Q, crystalline B4T13 ($Q\cdot f_r$=8,000 GHz [31,40]) and BTB ($Q\cdot f_r$=23,000 GHz [42]) phases. Results of temperature coefficient of resonant frequency (τ_f) are summarized in Fig. 10(C), which varies in the range of 20–40 ppm/°C, and exhibits an increasing trend with CB or BCB content. This might be related to the formation of BT5 and B4T13 phases (Fig. 7), because both of them have a τ_f in the range of 40–50 ppm/°C [39,40], larger than that of BT4, 20 ppm/°C [22].

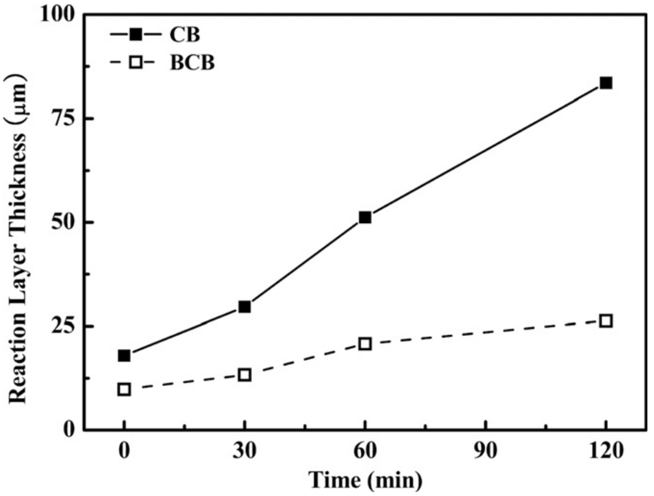

Fig. 9. Reaction layer thickness on BT4 side as a function of time for CB/BT4 and BCB/BT4 diffusion couples fired at 925 °C.

4. Conclusions

By adding a crystalline phase of CuB_2O_4 (CB) or $BaCuB_2O_5$ (BCB), the $BaTi_4O_9$ (BT4) can be densified at 900–925 °C, which is 400–450 °C, lower than that required for pure BT4. Faster and larger densification kinetics is observed in the system of CB+BT4 than BCB+BT4.

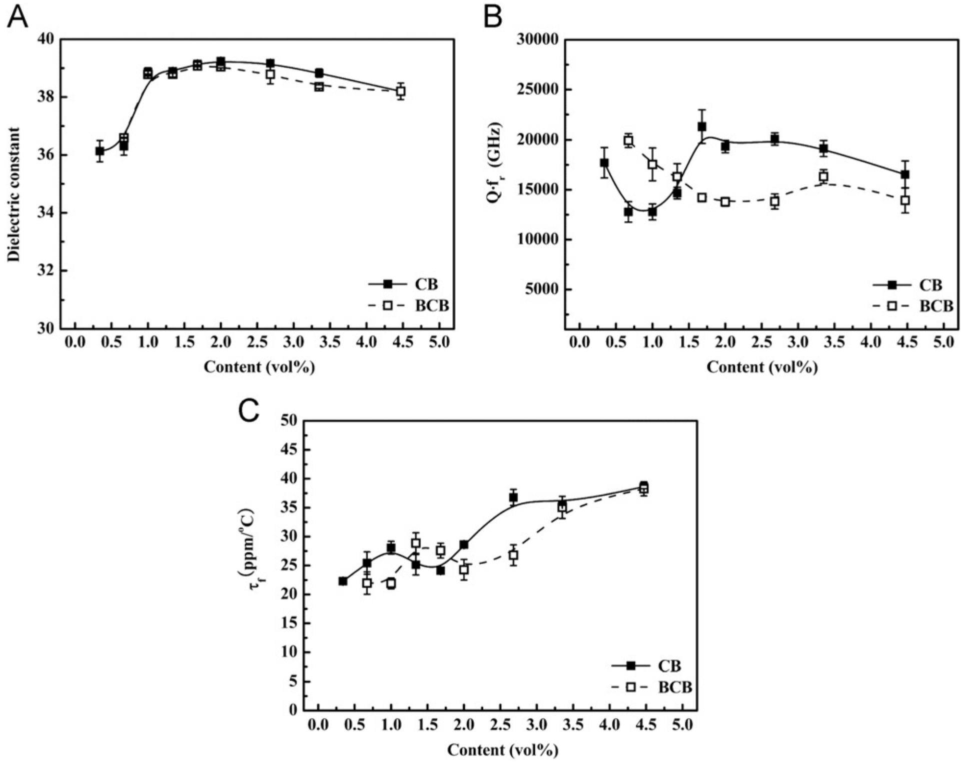

Fig. 10. (A) Dielectric constant (k), (B) $Q\cdot f_r$, and (C) temperature coefficient of resonant frequency (τ_f) at 6.6 GHz for BT4 with different amounts of CB and BCB fired at 925 °C, for 2 h.

This attributed to an interfacial reaction taking place at the interface of CB/BT4, which becomes less significant with BaO present in BCB. For the samples with 0.34–4.47 vol% CB or BCB, the resulting binary microwave ceramic composites have a dielectric constant of 36–40, a $Q \cdot f_r$ value of 13,000–21,000 GHz at 6.6 GHz and a temperature coefficient of resonant frequency (τ_f) of 20–40 ppm/°C in the temperature range of 25–80 °C.

Acknowledgments

Funding for this study has been provided by the National Science Council of the Republic of China under Grant no–99-2221-E-007-036-MY3.

References

[1] D.M. Mattox, S.R. Gurkovich, J.A. Olenick, K.M. Mason, Low dielectric constant, alumina-compatible, Co-fired multilayer substrate, Ceramic Engineering and Science Proceedings 9 (1988) 1567–1578.

[2] N. Niwa, N. Kamehara, H. Yokoyama, K. Yokouchi, K. Kurihara, Multilayer ceramic circuit board with copper conductor, in: J.B. Blum, W.R. Cannon (Eds.), Advances in Ceramics, vol. 19, American Ceramic Society, Westerville, OH, 1986, pp. 41–47.

[3] T.K. Gupta, J.H. Jean, Principles of the development of a silica dielectric for microelectronic packaging, Journal of Materials Research 11 (1996) 243–263.

[4] S.H. Knickerbocker, A.H. Kumar, L.W. Herron, Cordierite glass-ceramics for multilayer ceramic packaging, American Ceramic Society Bulletin 72 (1993) 90–95.

[5] R.R. Tummala, Ceramic and glass-ceramic packaging in the 1990s, Journal of the American Ceramic Society 74 (1991) 895–908.

[6] C.R. Chang, J.H. Jean, Crystallization kinetics and mechanism of low-dielectric, low-temperature cofirable $CaO–B_2O_3–SiO_2$ glass-ceramics, Journal of the American Ceramic Society 82 (1999) 1725–1732.

[7] J.H. Jean, Y.C. Fang, S.X. Dai, R.F. Huang, D.L. Wilcox Sr., Devitrification kinetics and mechanism of $K_2O–CaO–SrO–BaO–B_2O_3–SiO_2$, Journal of the American Ceramic Society 84 (2001) 1354–1360.

[8] M. Udovic, M. Valant, D. Suvorov, Phase formation and dielectric characterization of the $Bi_2O_3–TeO_2$ system prepared in an oxygen atmosphere, Journal of the American Ceramic Society 87 (2004) 591–597.

[9] M. Udovic, M. Valant, D. Suvorov, Dielectric characterisation of ceramics from the $TiO_2–TeO_2$ system, Journal of the European Ceramic Society 21 (2001) 1735–1738.

[10] D.K. Kwon, M.T. Lanagan, T.R. Shrout, Microwave dielectric properties of $BaO–TeO_2$ binary compounds, Materials Letters 61 (2007) 1827–1831.

[11] D.K. Kwon, M.T. Lanagan, T.R. Shrout, Synthesis of $BaTiTe_3O_9$ ceramics for LTCC application and its dielectric properties, Journal of the Ceramic Society of Japan 113 (3) (2005) 216–219.

[12] A. Feteira, D.C. Sinclair, Microwave dielectric properties of low firing temperature $Bi_2W_2O_9$ ceramics, Journal of the American Ceramic Society 91 (4) (2008) 1338–1341.

[13] M. Valant, D. Suvorov, Glass-free low-temperature co-fired ceramics: calcium germanates, silicates and tellurates, Journal of the European Ceramic Society 24 (2004) 1715–1719.

[14] G. Subodh, M.T. Sebastian, Glass-free $Zn_2Te_3O_8$ microwave ceramic for LTCC, Journal of the American Ceramic Society 90 (7) (2007) 2266–2268.

[15] D. Zhou, H. Wang, X. Yao, L.-X. Pang, Microwave dielectric properties of low temperature firing $Bi_2Mo_2O_9$ ceramic, Journal of the American Ceramic Society 91 (10) (2008) 3419–3422.

[16] D. Zhou, H. Wang, L.-X. Pang, C.A. Randall, X. Yao, $Bi_2O_3–MoO_3$ binary system: an alternative ultralow sintering temperature microwave dielectric, Journal of the American Ceramic Society 92 (10) (2009) 2242–2246.

[17] D.K. Kwon, M.T. Lanagan, T.R. Shrout, Microwave dielectric properties and low-temperature cofiring of $BaTe_4O_9$ with aluminum metal electrode, Journal of the American Ceramic Society 88 (2005) 3419–3422.

[18] H.M. O'Bryan, J. Thomson, J.K. Plourde, A new $BaO–TiO_2$ compound with temperature-stable high permittivity and low microwave loss, Journal of the American Ceramic Society 57 (1974) 450–453.

[19] S.G. Mhaisalkar, W.E. Lee, D.W. Readey, Processing and characterization of $BaTi_4O_9$, Journal of the American Ceramic Society 72 (1989) 2154–2158.

[20] H.M. O'Bryan, J. Thomson, Phase equilibria in the TiO_2-rich region of the system $BaO–TiO_2$, Journal of the American Ceramic Society 57 (1974) 522–526.

[21] S.G. Mhaisalkar, D.W. Readey, S.A. Akbar, Microwave dielectric properties of doped $BaTi_4O_9$, Journal of the American Ceramic Society 74 (1991) 1894–1898.

[22] J.H. Choy, Y.S. Han, Microwave characteristics of $BaO–TiO_2$ ceramics prepared via a citrate route, Journal of the American Ceramic Society 78 (1995) 1167–1172.

[23] M.H. Weng, T.J. Liang, C.L. Huang, Lowering of sintering temperature and microwave dielectric properties of $BaTi_4O_9$ ceramics prepared by the polymeric precursor method, Journal of the European Ceramic Society 22 (2002) 1693–1698.

[24] C.F. Yang, The microwave characteristics of glass-$BaTi_4O_9$ ceramics, Japanese Journal of Applied Physics 38 (1999) 3576–3579.

[25] D.W. Kim, D.G. Lee, K.S. Hong, Low-temperature firing and microwave dielectric properties of $BaTi_4O_9$ with Zn–B–O glass system, Materials Research Bulletin 36 (2001) 585–595.

[26] S.G. Lu, K.W. Kwok, H.L. Chan, C.L. Choy, Structural and electrical properties of $BaTi_4O_9$ microwave ceramics incorporated with glass phase, Materials Science and Engineering B99 (2003) 491–494.

[27] C.M. Cheng, C.F. Yang, S.H. Lo, T.Y. Tseng, Sintering $BaTi_4O_9/Ba_2Ti_9O_{20}$-based ceramics by glass addition, Journal of the European Ceramic Society 20 (2000) 1061–1067.

[28] T. Takada, S.F. Wang, S. Yoshikawa, S.J. Jang, R.E. Newnham, Effect of glass addition on $BaO–TiO_2–WO_3$ microwave ceramics, Journal of the American Ceramic Society 77 (1994) 1909–1916.

[29] T. Takada, S.F. Wang, S. Yoshikawa, S.J. Jang, R.E. Newnham, Evolution of interfacial microstructure between barium titanate and binary glass, Journal of the American Ceramic Society 77 (1994) 852–856.

[30] M.Z. Jhou, J.H. Jean, Low-fire processing of microwave $BaTi_4O_9$ with $BaO–ZnO–B_2O_3$ glass, Journal of the American Ceramic Society 89 (2006) 786–791.

[31] J.B. Lim, M.H. Kim, J.C. Kim, S. Nahm, J.H. Paik, J.H. Kim, Effect of $BaCuB_2O_5$ additive on the sintering temperature and microwave dielectric properties of $BaTi_4O_9$ ceramics, Japanese Journal of Applied Physics 45 (2006) 242–244.

[32] Y.J. Choi, J.H. Park, W.J. Ko, J.H. Park, S. Nahm, J.G. Park, Low temperature sintering of $BaTi_4O_9$-based middle-k dielectric composition for LTCC applications, Journal of Electroceramics 14 (2005) 157–162.

[33] Y.L. Tung, J.H. Jean, Chemical synthesis of a blue-emitting $NaSr_{1-X}PO_4{:}Eu_X$ phosphor powder, Journal of the American Ceramic Society 92 (2009) 1860–1862.

[34] B.W. Hakki, P.D. Coleman, A dielectric resonator method of measuring inductive capacities in the millimeter range, IEEE Transactions on Microwave Theory and Techniques **MTT-**8 (1960) 402–410.

[35] Y. Kobayashi, M. Katoh, Microwave measurement of dielectric properties of low-loss materials by the dielectric rod resonator

method, IEEE Transactions on Microwave Theory and Techniques **MTT-**33 (1985) 586–592.

[36] N.S. Shuster, L.K. Zeinalova, M.I. Zargarova, B_2O_3–CuO system, Russian Journal of Inorganic Chemistry 35 (1990) 151–152.

[37] M.H. Kim, J.B. Lim, J.C. Kim, S. Nahm, J.H. Paik, J.H. Kim, K.S. Park, Synthesis of $BaCuB_2O_5$ ceramics and their effect on the sintering temperature and microwave dielectric properties of $Ba(Zn_{1/3}Nb_{2/3})O_3$ ceramics, Journal of the American Ceramic Society 89 (2006) 3124–3128.

[38] T. Negas, G. Yeager, S. Bell, N. Coats, I. Minis, $BaTi_4O_9/Ba_2Ti_9O_{20}$-based ceramics resurrected for modern microwave applications, Journal of American Ceramic Society Bulletin 72 (1993) 80–89.

[39] S. Hirano, T. Hayashi, K. Kikuta, J. Otsuka, chemical processing and properties of $BaTi_5O_{11}$ microwave dielectrics, Ceramic Transactions 12 (1990) 733–740.

[40] J.B. Lim, S. Nahm, H.T. Kim, J.H. Kim, J.H. Paik, H.J. Lee, Effect of B_2O_3 and CuO on the sintering temperature and microwave dielectric properties of the $BaTi_4O_9$ ceramics, Journal of Electroceramics 17 (2006) 393–397.

[41] J.K. Plourde, D.F. Linn, H.M. O'Bryan Jr., J. Thomson Jr., $Ba_2Ti_9O_{20}$ as a microwave dielectric resonator, Journal of the American Ceramic Society 58 (1975) 418–420.

[42] W. Huang, K.S. Liu, L.W. Chu, G.H. Hsu, I.N. Lin, Microwave dielectric properties of LTCC materials consisting of glass–$Ba_2Ti_9O_{20}$ composites, Journal of the European Ceramic Society 23 (2003) 2559–2563.